Metabolic changes following Primary SIV-Infection in Rhesus Macaques: 3D multivoxel Proton MR Spectroscopy at 3 T

William E. Wu[1], Assaf Tal[1], Ivan Kirov[1], Henry Rusinek[1], James Babb[1], Eva-Maria Ratai[2], Chan-Gyu Joo[2], R Gilberto Gonzalez[2], and Oded Gonen[1]

[1]Radiology, New York University School of Medicine, New York, NY, United States, [2]Neuroradiology, Athinoula A. Martinos Center for Biomedical Imaging and Neuroradiology, Charlestown, MA, United States

Introduction: Because of its similar pathogenesis, the simian immunodeficiency virus (SIV)-infected rhesus macaque is often used as an animal model for human HIV-infection. Although several proton MR spectroscopy (^{1}H-MRS) studies have been reported using such models (1-3), all used low, 1-3 cm^3 spatial resolution (relative to the ~80 cm^3 brain) single voxels placed in few brain regions. Consequently, the relative dysfunction of global gray and white matter (GM, WM) remains unknown. To assess this SIV-related diffuse dysfunction, we performed three-dimensional (3D) multivoxel ^{1}H-MRS imaging (MRSI) over extensive, 28 cm^3 (~35%) of the macaque brain at 0.125 cm^3 spatial resolution and compared the absolute *N*-acetylaspartate (NAA), creatine (Cr), choline (Cho), and myo-inositol (mI) concentrations in five rhesus macaques at baseline and 4-6-weeks post-infection. To ascertain global GM and WM metabolism, we segmented the animals' T2-weighted MRI into these tissue components and overlaid them onto metabolic maps generated from spectral modeling to calculate absolute metabolite concentrations within each tissue type.

Methods: All experiments were done in a 3-T MR imager (Magnetom TIM Trio, Siemens AG, Erlangen, Germany) with a circularly-polarized transmit-receive human knee coil. To guide placement of the ^{1}H-MRS volume-of-interest (VOI), sagittal and axial turbo spin echo MRIs (TE/TR=16/7430 ms, 140×140 mm^2 field-of-view (FOV), 512×512 matrix, 2.0 mm sagittal and 1.2 mm axial slice thickness) were acquired. A 4.0 cm anterior-posterior (AP) × 3.5 cm left-right (LR) × 2.0 cm inferior-superior (IS) =28 cm^3 ^{1}H-MRSI VOI was then centered on the corpus callosum. The VOI was excited using PRESS (TE/TR=33/1440 ms) with two 2nd-order Hadamard encoded slabs (4 slices) interleaved within every TR. These slices' planes were encoded with 16×16 2D-CSI over an 8×8 cm^2 (LR×AP) FOV to yield nominal (0.5 cm)^3 voxels, 224 of which fell within the VOI. These 224 VOI spectra were each frequency-aligned and zero-order phased in reference to the NAA peak, then summed, retaining individual spectra linewidth and improved SNR by $224^{½} \approx 15$-fold. Relative levels of the i^{th} (NAA, Cr, Cho, *m*I) metabolite in the k^{th} animal were estimated from their peak areas, S_{ik}, using parametric spectral modeling and least-squares optimization software of Soher *et al.* (4). The S_{ik} were recorded into metabolic maps for each animal, then scaled into absolute concentrations by phantom replacement as described previously (5). Five (3 females, 2 males; 5.0–8.6 kg weight) healthy 3–4 year old adult rhesus macaques were scanned, then infected by intravenous injection with SIV, and finally rescanned 4-6 weeks later. Animals were under constant veterinary supervision. The protocol was approved by both the Harvard Medical School and Massachusetts General Hospital IACUCs. To determine global GM and WM metabolism, T2-weighted images were segmented using our FireVoxel package (6). Segmented components (GM, WM, CSF) were then co-registered with spectrally modeled metabolic maps for each animal using in-house software written in MATLAB 2009b (The Mathworks Inc., Natick, MA). The software estimated partial volume contributions in every voxel and calculated global GM and WM metabolite concentrations.

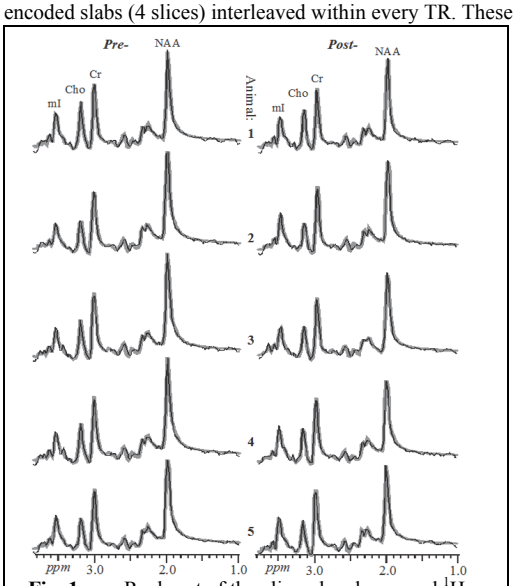

Fig. 1. Real part of the aligned and summed ^{1}H spectra from all 224 voxels in the VOI (thin black lines), for each of the 5 animals pre- (left) and post-SIV infection, superimposed with the sum of the fitted model functions (thick gray lines). All are on common intensity and chemical shift scales. Note the excellent ~140–390 SNRs and spectral resolution.

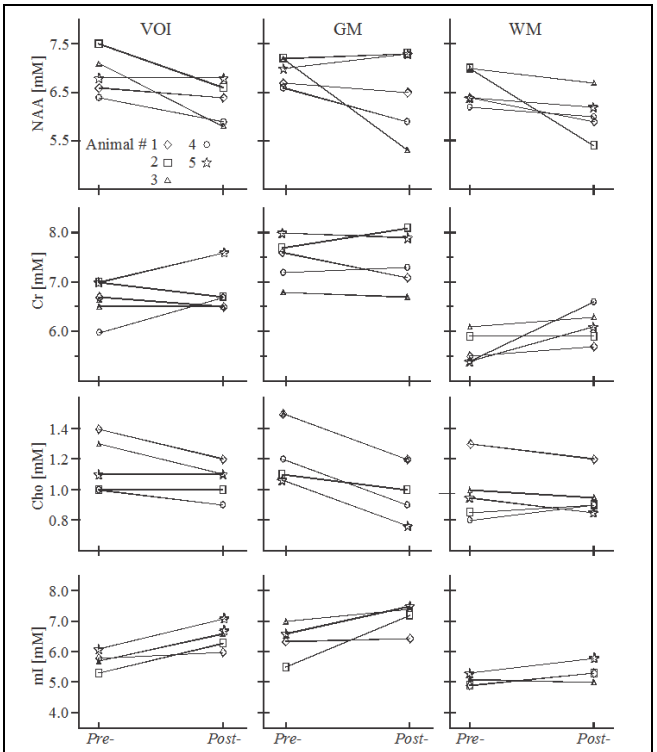

Fig. 2. Line plots of the NAA, Cr, Cho and mI concentrations for all macaques, at healthy baseline and 4-6 weeks after SIV-infection, for each tissue compartment (all-tissue VOI, GM, WM). Note the significant (›10%) declines in VOI and GM Cho, elevation in VOI mI, and marked declines in both VOI and WM NAA.

Results: Sums of all 224 VOI spectra for each animal *pre*- and *post*-infection, overlaid with the sums of their fits, are shown in **Fig. 1**. They demonstrate SNRs (mean±standard deviation) of 390±30, 223±12, 151±17 and 144±17 for NAA, Cr, Cho and *m*I. **Fig. 2** shows the change in mean absolute metabolite concentrations after SIV infection compared to baseline. It reveals a significant global VOI 13% decline in Cho (1.2±0.2 to 1.0±0.1 millimoles/g (mM) wet weight; p‹0.03) and 11% increase in mI (5.7 ±0.4 to 6.5±0.5 mM; p‹0.03). A significant 20% Cho decline (1.3±0.2 to 1.0±0.1 mM; p‹0.003) was found only in GM. We also found a significant 9% average NAA decline in the VOI (6.9±0.5 to 6.3±0.4 mM; p‹0.04) and 8% average NAA decline in the WM (6.6±0.4 to 6.0±0.5 mM; p=0.05), but no significant change in GM.

Discussion: The 3D ^{1}H-MRS changes observed here are consistent with previous studies (7) indicating initially elevated Cho levels revert back to baseline or below after the first month of infection, especially in GM areas such as the basal ganglia, suggesting a possible host immunological response. However, NAA declines and mI elevation suggest a complex pattern of disease response involving neuronal injury/loss and astrogliosis which is not yet fully understood. These 3D MRSI changes may serve as valuable metabolic markers of diffuse disease-related change and provide information on specific GM- and/or WM-related activity during the primary stages of disease.

References: (1) Greco J *et al, MRM* 2004 (2) Ratai EM *et al, BMC Neurosci* (3) Williams K *et al, J Clin Invest* 2005 (4) Soher BJ *et al, MRM* 1998 (5) Inglese M *et al, MRM* 2003 (6) Mikheev *et al, J MRI* 2008 (7) Fuller RA *et al, BMC Neurosci* 2004